Cooperative Localization for Autonomous Underwater Vehicles

Alexander Bahr, John J. Leonard, Maurice F. Fallon

Abstract

This paper describes an algorithm for distributed acoustic navigation for Autonomous Underwater Vehicles (AUVs). Whereas typical AUV navigation systems utilize pre-calibrated arrays of static transponders, our work seeks to create a fully mobile network of AUVs that perform acoustic ranging and data exchange with one another to achieve cooperative positioning for extended duration missions over large areas. The algorithm enumerates possible solutions for the AUV trajectory based on dead-reckoning and range-only measurements provided by acoustic modems that are mounted on each vehicle, and chooses the trajectory via minimization of a cost function based on these constraints. The resulting algorithm is computationally efficient, meets the strict bandwidth requirements of available AUV modems, and has potential to scale well to networks of large numbers of vehicles. The method has undergone extensive experimentation, and results from three different scenarios are reported in this paper, each of which utilizes MIT SCOUT Autonomous Surface Craft (ASC) as convenient platforms for testing. In the first experiment, we utilize three ASCs, each equipped with a Woods Hole acoustic modem, as surrogates for AUVs. In this scenario, two ASCs serve as Communication/Navigation Aids (CNAs) for a third ASC that computes its position based exclusively on GPS positions of the CNAs and acoustic range measurements between platforms. In the second scenario, an undersea glider is used in conjunction with two ASCs serving as CNAs. Finally, in the third experiment, a Bluefin12 AUV serves as the target vehicle. All three experiments demonstrate the successful operation of the technique with real ocean data.

Index Terms

autonomous underwater vehicles, cooperative navigation, mobile robotics, sensor networks

I. Introduction

The absence of Global Positioning System (GPS) signals underwater makes navigation for Autonomous Underwater Vehicles (AUVs) a difficult challenge. Without an external reference in the form of acoustic beacons at known positions, the vehicle has to rely on proprioceptive information obtained through a compass, a Doppler Velocity Logger (DVL) or an Inertial Navigation System (INS) [WYSH00]. Independent of the quality of the sensors used, the error in the position estimate based on dead-reckoning information grows without bound. Typical navigation

The authors are with the Computer Science and Artificial Intelligence Laboratory, Massachusetts Institute of Technology, Cambridge, MA 02139, USA

errors are 0.5 % to 2 % of distance traveled for vehicles operating within a few hundred meters of the sea floor such that their DVL has a lock on the bottom. Errors as low as 0.1 % can be obtained with large and expensive INS systems, but for vehicles relying only on a compass and a speed estimate, errors can be as high as 20 %. By surfacing the AUV can obtain a position update through its GPS, but this is impossible (under ice) or undesirable for many applications. The use of static beacons in the form of a Long Baseline (LBL) array limits the operation area to a few km^2 and requires a substantial deployment effort before operations, especially in deep water.

As underwater vehicles become more reliable and affordable the simultaneous use of several AUVs recently became a viable option and multi-vehicle deployments will become standard in the upcoming years. This will not only make possible entirely new types of missions which rely on cooperation, but will also allow each individual member of the group to benefit from navigation information obtained from other members. For optimal cooperative localization a few dedicated Communication and Navigation Aid-AUVs (CNAs), which maintain an accurate estimate of their position through sophisticated DVL and INS sensors, can enable a much larger group of vehicles with less sophisticated navigation suites to maintain an accurate position, as described in [VLCW04a].

The idea of an underwater equivalent to the terrestrial GPS has long held appeal to AUV researchers. For example, A.C.S.A. has developed a portable undersea tracking range that provides a form of “underwater GPS” in a local area [Tho01]. In the A.C.S.A. system, a network of four surface buoys equipped with GPS and RF communications utilize passive acoustic range measurements to track the position of a time-synchronized mobile undersea device. While the base system usually employs moored or drifted surface buoys, experiments using self-powered surface craft have also been performed. Further extensions of this concept could employ acoustic communications to relay the vehicle pose estimate obtained by the surface buoys back to the undersea vehicle itself.

The motivation behind our research is to enable multiple AUVs to cooperatively navigate. The ideal solution would enable heterogeneous teams of AUVs to operate with high navigational precision, without frequent surfacing for GPS measurements, even for the case when only a small number of the AUVs in the team are equipped with expensive inertial sensors. One application of this capability would be to perform rapid, large-area search with a mixed AUV network consisting of Comm/Nav-Aid AUVs, Search-Classify-Map AUVs, and Reacquire-Identify AUVs [VLCW04b].

The problem of cooperative navigation of AUVs is highly interconnected to the problem of undersea acoustic communications [Cat90], [KB00], [FJG+01]. Our work capitalizes on recent progress by the Acoustic Modem Group at Woods Hole Oceanographic Institution (WHOI) in developing integrated communication and navigation (ranging) capabilities for small AUVs. This application raises several interesting challenges for acoustic telemetry research, such as the need to handle a fully mobile network and the goal of achieving accurate one-way ranging through stable clock synchronization.

There has been a great deal of work in terrestrial settings on the problem of cooperative navigation of multiple mobile robots. Often the problem is cast in terms of a mix of mobile and static nodes in a large-scale sensor network, with either angle-only or range-only measurements. A variety of state estimation approaches have been followed, including Markov chain Monte Carlo and set-theoretic state estimators. For example, Liao et al. [LHDS06]

employed a particle filter state estimator for cooperative localization of multiple ground robots using range-only measurements. Djugash et al. [DKSZ06] developed an approach that integrated Simultaneous Localization and Mapping (SLAM) with mobile sensor networks, achieving self-calibration of a network consisting of mobile and stationary nodes with range measurements. Grocholsky et al. [GSSK06] used nonlinear set-based state estimation techniques for localization of multiple mobile robots with range measurements between platforms.

The underwater setting presents some unique challenges for cooperative mobile robotics. The assumption of a fast and reliable communication channel between all participants of the cooperative navigation effort, as made in [RB00], [RDM02], and [MLRT04], does not hold underwater. Due to the strong attenuation of electro-magnetic waves underwater, radio or optical communication is not practically feasible except for distances of a few meters. As a result acoustic modems, typically operating between 15 and 30 kHz, provide the only possible means of communicating at long ranges underwater. Data rates are typically several orders of magnitude below those achieved with radio-based communication channels [KB00]. With sound propagation being dependent on temperature and salinity, which can both vary strongly within the water column, the acoustic communication channel is unreliable and its performance hard to predict. This is especially true in shallow water, where severe multi-path is often encountered. The concept of portable landmarks as outlined in [KNH94] is not feasible as it is often difficult for an AUV to hold its position, especially in strong currents.

The objective for our work is to develop and test an algorithm for cooperative positioning of multiple mobile undersea vehicles that can use acoustic modems concurrently for both ranging and for communication [FJG+01]. The solution must be robust to the errors and time delays that are inherent to acoustic range measurements and must take into account the severe bandwidth constraints of state-of-the-art undersea acoustic modems. This restriction prevents the transfer of full state information between vehicles.

The cooperative navigation problem is complementary to the problems of cooperative motion planning and control for underwater platforms. For example, Leonard et al. have addressed a class of cooperative adaptive sampling problems for networks of AUVs and underwater gliders [LPL+07]. In this work the motion of a fleet of vehicles is directed to acquire optimal data sets based on the predictions of numerical ocean models. This work typically assumes that accurate navigation information is available, for example through GPS measurements obtained at the surface. This scenario provides a compelling application scenario in which our cooperative navigation techniques could be applied, obviating the need for all vehicles in the fleet to surface for positioning.

Using a one-way messaging system with the WHOI modem, Eustice et al. [EWSG07] recently implemented a least squares version of a maximum likelihood algorithm to carry out moving baseline navigation. The approach utilized a particularly accurate heading and dead-reckoning system and as well as a specially designed low drift timing clock.

II. Technical Approach

In order to cooperate during their mission the AUVs will be outfitted with acoustic modems. Data rates on the order of 100 bytes/s over distances of up to 5 km have been achieved, but given varying channel quality,

multi-path propagation and possible interference with other acoustic sources, these can drop to as low as 32 byte data packets sent every ten seconds. Furthermore, the small bandwidth of the frequency spectrum which is usable for acoustic communication restricts the use of Frequency-Division-Multiple-Access (FDMA) schemes for multiple channels. The modem which is used throughout these experiments has been developed by the Acoustics Group at WHOI [FJG$^+$01]. A special feature of this modem is its ability to embed a time stamp into the data packet and transmit messages which are synced to a pulse-per-second (PPS) signal if such a signal is provided. This signal can be obtained from a GPS receiver and thereby allows all modems to be synced to the same global reference clock. When the AUV is submerged and no GPS is available, the PPS signal is obtained from a precise timer which is synchronized to the GPS clock at the surface [EWSG07]. If the transmitting and receiving modem have a PPS signal the receiving modem knows when the message has been sent. This feature is particularly useful for cooperative navigation as each listener overhearing a transmitted data package can now estimate its distance to the transmitting vehicle based on the time of flight (TOF).

In general, any asset in the water outfitted with an acoustic modem (AUV, ship, ASC, fixed mooring) can participate actively (by transmitting navigation information) or passively (by receiving). We assume, however, for the remaining discussion that an AUV navigates by receiving multiple messages from a CNA. It is important to note that it does not matter if the transmissions are all sent by the same CNA or each time by a different one. The localization algorithm is decentralized and each node incorporates every overheard data packet which contains an estimate of the transmitting vehicle's position (latitude, longitude and depth) as well as uncertainty information. Assuming that most data packets transmitted contain this information, it is not necessary to transmit data packets dedicated to cooperative navigation, which is crucial given the small available bandwidth.

A. The Cooperative Navigation Algorithm

With each successful transmission at time k the AUV receives an estimate of the CNA's position $\boldsymbol{x}^C(k) = [x^C(k), y^C(k)]^T$, the covariance matrix, $\boldsymbol{P}^C(k)$, which accounts for the confidence the CNA has in each component of $\boldsymbol{x}^C(k)$, a depth $z^C(k)$ and the range $r(k)$ between the AUV and the CNA.

$$\boldsymbol{P}^C(k) = \begin{bmatrix} {\sigma_{xx}^C}^2(k) & {\sigma_{xy}^C}^2(k) \\ {\sigma_{yx}^C}^2(k) & {\sigma_{yy}^C}^2(k) \end{bmatrix}$$

$\boldsymbol{x}^C(k)$ and $\boldsymbol{P}^C(k)$ can be a snapshot from the navigation filter running on the CNA or from the GPS in case the CNA is at the surface. The range $r(k)$ is directly obtained by the AUV through the PPS-synced transmission feature. Many experiments have shown that the error in the range measurement $r(k)$ is only weakly range-dependent and can be modeled as a Gaussian with mean $r(k)$ and a fixed variance σ_r^2. As depth can be accurately measured with a pressure sensor, the AUV can use its depth $z^A(k)$ and the depth received from the CNA $z^C(k)$ to project the CNA's position into a 2D plane at $z^A(k)$ and thereby reducing the cooperative localization from a 3D to a 2D problem.

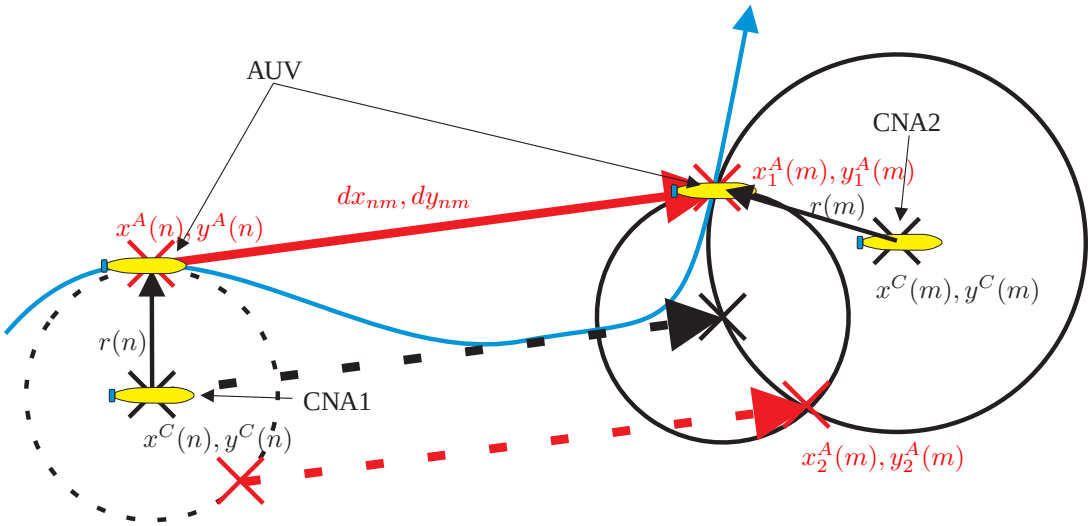

Fig. 1: Computing two possible positions of the AUV at $t(m)$ ($x_1^A(m), y_1^A(m)$ and $x_2^A(m), y_2^A(m)$) using the dead-reckoning information dx_{nm}, dy_{nm} and the information $x^C(n), y^C(n)$ and $r(n)$ received at $t(n)$ from CNA1 and $x^C(m), y^C(m)$ and $r(m)$ received at $t(m)$ from CNA2

Furthermore, the AUV builds a matrix $\boldsymbol{D}$ where each entry $\boldsymbol{D}(n,m)$ contains the distance traveled $\boldsymbol{d}_{\overline{n,m}} = [dx_{\overline{n,m}}, dy_{\overline{n,m}}]^T$ between receiving a transmission at $t(n)$ and at $t(m)$ as obtained from proprioceptive measurements as well as the covariance matrix $\boldsymbol{Q}_{\overline{n,m}}$ associated with that measurement.

$$\boldsymbol{Q}_{\overline{n,m}} = \begin{bmatrix} {\sigma_{dx_{\overline{n,m}}}}^2 & 0 \\ 0 & {\sigma_{dy_{\overline{n,m}}}}^2 \end{bmatrix}$$

Figure 1 shows how the AUV uses information received at $t(n)$ and $t(m)$ to compute two possible solutions for its position at $t(m)$: The circle with radius $r(n)$ defines all possible positions at $t(n)$. Shifting the center of this circle by $[dx_{n,m}, dy_{n,m}]^T$ and solving the resulting quadratic equation, we obtain a set $\boldsymbol{X}^A(m)$ of 0, 1 or 2 intersections with the circle around $\boldsymbol{x}^C(m)$ with radius $r(m)$.

$$\boldsymbol{X}^A(m) = \mathcal{F}(\boldsymbol{x}(n)^C, \boldsymbol{x}(m)^C, r(n), r(m), \boldsymbol{d}_{\overline{n,m}}) \tag{1}$$

with

$$\boldsymbol{X}^A(m) = \emptyset \quad \text{or} \quad \boldsymbol{X}^A(m) = \boldsymbol{x}_1^A(m) \quad \text{or} \quad \boldsymbol{X}^A(m) = \begin{pmatrix} \boldsymbol{x}_1^A(m) \\ \boldsymbol{x}_2^A(m) \end{pmatrix}$$

Using other values for n ($n = [1, \ldots, m-1]$), we can compute up to $2(m-1)$ solutions for $\boldsymbol{x}^A(m)$. For the upcoming computations we assume that we use q solutions. The Jacobian of the intersection function $\mathcal{F}$ with respect to the measured and transmitted parameters $\boldsymbol{x}^C(n)$, $\boldsymbol{x}^C(m)$, $r(n)$, $r(m)$, $\boldsymbol{d}_{\overline{n,m}}$ is $\boldsymbol{J}_{n,m}$ and can be used to compute $\boldsymbol{P}^A(m)$ the covariance of $\boldsymbol{x}^A(m)$. $\boldsymbol{P}^A(m)$ is given by

$$\boldsymbol{P}^A(m) = \begin{bmatrix} {\sigma_{xx}^A}^2(m) & {\sigma_{xy}^A}^2(m) \\ {\sigma_{yx}^A}^2(m) & {\sigma_{yy}^A}^2(m) \end{bmatrix} = \boldsymbol{J}_{n,m}\boldsymbol{G}_{n,m}\boldsymbol{J}_{n,m}^T \tag{2}$$

with

$$\boldsymbol{G}_{n,m} = \begin{bmatrix} {\sigma_{xx}^C}^2(n) & {\sigma_{xy}^C}^2(n) & 0 & 0 & 0 & 0 & 0 & 0 \\ {\sigma_{yx}^C}^2(n) & {\sigma_{yy}^C}^2(n) & 0 & 0 & 0 & 0 & 0 & 0 \\ 0 & 0 & {\sigma_{xx}^C}^2(m) & {\sigma_{xy}^C}^2(m) & 0 & 0 & 0 & 0 \\ 0 & 0 & {\sigma_{yx}^C}^2(m) & {\sigma_{yy}^C}^2(m) & 0 & 0 & 0 & 0 \\ 0 & 0 & 0 & 0 & {\sigma_r}^2(n) & 0 & 0 & 0 \\ 0 & 0 & 0 & 0 & 0 & {\sigma_r}^2(m) & 0 & 0 \\ 0 & 0 & 0 & 0 & 0 & 0 & {\sigma_{dx}}^2(n,m) & 0 \\ 0 & 0 & 0 & 0 & 0 & 0 & 0 & {\sigma_{dy}}^2(n,m) \end{bmatrix}$$

and

$$\boldsymbol{J}_{n,m} = \begin{bmatrix} \frac{\partial x^A(m)}{\partial x^C(n)} & \frac{\partial x^A(m)}{\partial y^C(n)} & \frac{\partial x^A(m)}{\partial x^C(m)} & \frac{\partial x^A(m)}{\partial y^C(m)} & \frac{\partial x^A(m)}{\partial r(n)} & \frac{\partial x^A(m)}{\partial r(m)} & \frac{\partial x^A(m)}{\partial dx_{n,m}} & \frac{\partial x^A(m)}{\partial dy_{n,m}} \\ \frac{\partial y^A(m)}{\partial x^C(n)} & \frac{\partial y^A(m)}{\partial y^C(n)} & \frac{\partial y^A(m)}{\partial x^C(m)} & \frac{\partial y^A(m)}{\partial y^C(m)} & \frac{\partial y^A(m)}{\partial r(n)} & \frac{\partial y^A(m)}{\partial r(m)} & \frac{\partial y^A(m)}{\partial dx_{n,m}} & \frac{\partial y^A(m)}{\partial dy_{n,m}} \end{bmatrix}$$

All possible solutions for $\boldsymbol{x}_v^A(m)$ and their respective covariances $\boldsymbol{P}_v^A(m)$ are combined into a matrix $\boldsymbol{S}(m)$, where v is the index for all solutions at time $t(m)$.

$$\boldsymbol{S}(m) = \begin{bmatrix} x_1^A(m) & y_1^A(m) & {\sigma_{1_{xx}}^A}^2(m) & {\sigma_{1_{xy}}^A}^2(m) & {\sigma_{1_{yx}}^A}^2(m) & {\sigma_{1_{yy}}^A}^2(m) \\ \vdots & \vdots & \vdots & \vdots & \vdots & \vdots \\ x_v^A(m) & y_v^A(m) & {\sigma_{v_{xx}}^A}^2(m) & {\sigma_{v_{xy}}^A}^2(m) & {\sigma_{v_{yx}}^A}^2(m) & {\sigma_{v_{yy}}^A}^2(m) \\ \vdots & \vdots & \vdots & \vdots & \vdots & \vdots \\ x_q^A(m) & y_q^A(m) & {\sigma_{q_{xx}}^A}^2(m) & {\sigma_{q_{xy}}^A}^2(m) & {\sigma_{q_{yx}}^A}^2(m) & {\sigma_{q_{yy}}^A}^2(m) \end{bmatrix}, \; v = [1 \dots q]$$

We also define a position matrix $\boldsymbol{T}(m-q)$ which stores all possible past positions of the AUV, going back to $t(m-q)$, i.e. $\boldsymbol{x}_u^A(m-o) \; ; \; \forall u = [1 \dots q], o = [1 \dots q]$, their respective covariances $\boldsymbol{P}_u^A(m-o)$ and an associated accumulated transition cost $c_u(m-o)$ at $t(m-o)$, where u indexes all possible positions, covariances and costs at $t(m-o)$.

$$\boldsymbol{T}(m-q) = \begin{bmatrix} x_1^A(m-1) & y_1^A(m-1) & {\sigma_{1_{xx}}^A}^2(m-1) & \dots & {\sigma_{1_{yy}}^A}^2(m-1) & c_1(m-1) \\ \vdots & \vdots & \vdots & \vdots & \vdots & \vdots \\ x_u^A(m-1) & y_u^A(m-1) & {\sigma_{u_{xx}}^A}^2(m-1) & \dots & {\sigma_{u_{yy}}^A}^2(m-1) & c_u(m-1) \\ \vdots & \vdots & \vdots & \vdots & \vdots & \vdots \\ x_q^A(m-1) & y_q^A(m-1) & {\sigma_{q_{xx}}^A}^2(m-1) & \dots & {\sigma_{q_{yy}}^A}^2(m-1) & c_q(m-1) \\ \vdots & \vdots & \vdots & \vdots & \vdots & \vdots \\ x_1^A(m-o) & y_1^A(m-o) & {\sigma_{1_{xx}}^A}^2(m-o) & \dots & {\sigma_{1_{yy}}^A}^2(m-o) & c_1(m-o) \\ \vdots & \vdots & \vdots & \vdots & \vdots & \vdots \\ x_u^A(m-o) & y_u^A(m-o) & {\sigma_{u_{xx}}^A}^2(m-o) & \dots & {\sigma_{u_{yy}}^A}^2(m-o) & c_u(m-o) \\ \vdots & \vdots & \vdots & \vdots & \vdots & \vdots \\ x_q^A(m-o) & y_q^A(m-o) & {\sigma_{q_{xx}}^A}^2(m-o) & \dots & {\sigma_{q_{yy}}^A}^2(m-o) & c_q(m-o) \\ \vdots & \vdots & \vdots & \vdots & \vdots & \vdots \\ x_1^A(m-q) & y_1^A(m-q) & {\sigma_{1_{xx}}^A}^2(m-q) & \dots & {\sigma_{1_{yy}}^A}^2(m-q) & c_1(m-q) \\ \vdots & \vdots & \vdots & \vdots & \vdots & \vdots \\ x_u^A(m-q) & y_u^A(m-q) & {\sigma_{u_{xx}}^A}^2(m-q) & \dots & {\sigma_{u_{yy}}^A}^2(m-q) & c_u(m-q) \\ \vdots & \vdots & \vdots & \vdots & \vdots & \vdots \\ x_q^A(m-q) & y_q^A(m-q) & {\sigma_{q_{xx}}^A}^2(m-q) & \dots & {\sigma_{q_{yy}}^A}^2(m-q) & c_q(m-q) \end{bmatrix}, \quad \begin{matrix} u = [1 \dots q] \\ o = [1 \dots q] \end{matrix}$$

If a known position $\boldsymbol{x}^A(0)$ (obtained on the surface through GPS) is available in the beginning it can be used to initialize $\boldsymbol{T}(0) = [\boldsymbol{x}^A(0) \;\; c(0) = 0]$. If no initial position is available, the first set of solutions $\boldsymbol{S}(0)$ initializes $\boldsymbol{T}(0)$ and position estimates become available when subsequent information packages are received.

Our cost function $\mathcal{C}_{u,v}(m-o,m)$ computes the cost (inverse of likelihood) of the AUV having traveled from $\boldsymbol{x}_u^A(m-o)$ to $\boldsymbol{x}_v^A(m)$ given $\boldsymbol{x}_u^A(m-o)$, $\boldsymbol{P}_u^A(m-o)$, $\boldsymbol{x}_v^A(m)$, $\boldsymbol{P}_v^A(m)$, $\boldsymbol{d}_{\overline{m-o,m}}$, $\boldsymbol{Q}_{\overline{m-o,m}}$.

This cost is expressed by the "distance" between $(\boldsymbol{x}_u^A(m-o) + \boldsymbol{d}_{\overline{m-o,m}})$, a solution at $t(m-o)$ forward propagated by the dead-reckoning information $\boldsymbol{d}_{\overline{m-o,m}})$, with the associated covariance $(\boldsymbol{P}_u^A(m-o) + \boldsymbol{Q}_{\overline{m-o,m}})$ and $\boldsymbol{x}_v^A$ a solution at $t(m)$ with the associated covariance $\boldsymbol{P}_v^A$. The distance metric used is the Kullback-Leibler divergence given by

$$\begin{aligned} \mathcal{C}_{u,v}(m-o,m) = \frac{1}{2}\Bigg(\ln\Bigg(\frac{det(\boldsymbol{P}_v^A)}{det(\boldsymbol{P}_u^A(m-o) + \boldsymbol{Q}_{\overline{m-o,m}})} \Bigg) + trace\big((\boldsymbol{P}_v^A)^{-1}(\boldsymbol{P}_u^A(m-o) + \boldsymbol{Q}_{\overline{m-o,m}})\big) \\ + \big(\boldsymbol{x}_v^A - (\boldsymbol{x}_u^A(m-o) + \boldsymbol{d}_{\overline{m-o,m}})\big)^T (\boldsymbol{P}_v^A)^{-1} \big(\boldsymbol{x}_v^A - (\boldsymbol{x}_u^A(m-o) + \boldsymbol{d}_{\overline{m-o,m}})\big) - 2 \Bigg) \end{aligned} \tag{3}$$

Using 3 we now compute the total cost $c_{u,v}(m-o,m)$ by computing the cost $\mathcal{C}_{u,v}(m-o,m)$ for all q^3 possible transitions from $\boldsymbol{T}(m-q)$ to $\boldsymbol{S}(m)$ and adding the new transition cost $\mathcal{C}_{u,v}(m-o,m)$ to the accumulated cost $c_u(m-o)$.

$$c_{u,v}(m-o,m) = \mathcal{C}_{u,v}(m-o,m) + c_u(m-o) \qquad \forall\, u=[1\dots q], v=[1\dots q], o=[1\dots q] \tag{4}$$

We then form a new position matrix $\boldsymbol{T}(m)$

$$\boldsymbol{T}(m) = \begin{bmatrix} x_1^A(m) & y_1^A(m) & {\sigma_{1_{xx}}^A}^2(m) & {\sigma_{1_{xy}}^A}^2(m) & {\sigma_{1_{yx}}^A}^2(m) & {\sigma_{1_{yy}}^A}^2(m) & c_1(m) \\ \vdots & \vdots & \vdots & \vdots & \vdots & \vdots & \vdots \\ x_v^A(m) & y_v^A(m) & {\sigma_{v_{xx}}^A}^2(m) & {\sigma_{v_{xy}}^A}^2(m) & {\sigma_{v_{yx}}^A}^2(m) & {\sigma_{v_{yy}}^A}^2(m) & c_v(m) \\ \vdots & \vdots & \vdots & \vdots & \vdots & \vdots & \vdots \\ x_q^A(m) & y_q^A(m) & {\sigma_{q_{xx}}^A}^2(m) & {\sigma_{q_{xy}}^A}^2(m) & {\sigma_{q_{yx}}^A}^2(m) & {\sigma_{q_{yy}}^A}^2(m) & c_q(m) \end{bmatrix},\ v=[1\dots q]$$

where $c_v(m)$ is the smallest accumulated cost associated with the transition to solution $\boldsymbol{x}_v^A(m)$ from of all q^2 possible positions $\boldsymbol{x}_u^A(m-o)$.

$$c_v(m) = \min_{\forall u}(c_{u,v}(m-o,m)) \qquad \forall\, v=[1\dots q], o=[1\dots q]. \tag{5}$$

All solutions $\boldsymbol{x}_v^A(m)$ are now hypotheses for possible positions of the AUV at $t(m)$ and weighted by the associated accumulated transition cost $c_v(m)$. The likeliest position $\boldsymbol{x}_w^A(m)$, i.e. our computed solution for $t(m)$ is the one with the smallest accumulated transition cost

$$\boldsymbol{x}_w^A(m) \text{ with } w \text{ s. t. } c_w(m) = \min_{\forall v}(c_v(m)) \tag{6}$$

B. Example

A single iteration of algorithm 1 is shown in the following example. Figure 2 shows a snapshot at $t(33)$ during a cooperative navigation experiment. The AUV (here simulated by an ASC which also provides GPS for ground-truth) has just received a position/range-pair from the CNA (full circle). This circle intersects with the position/range-pair received at $t(32)$ (dashed circle) and forward propagated by the dead-reckoned distance $\boldsymbol{d}_{\overline{32,33}}$ to $\boldsymbol{x}^C(32')$. It also intersects with other position/range-pairs received at $t(k), (1 \leq k < 32)$ (positions of CNA not shown) forward propagated to $\boldsymbol{x}^C(k')$ by the corresponding dead-reckoned distance $\boldsymbol{d}_{\overline{k,33}}$. All intersections and therefore possible solutions at $t(33)$ are shown with their corresponding accumulated transition cost. The inset in figure 2 shows the detailed view near the ground-truth (GPS) position. The computed position at $t(33)$ (marked with a large "X") is the one with the smallest accumulated transition cost selected out of all possible positions $\boldsymbol{x}_v^A(33)$. In this case it is not the one closest to the GPS-derived position.

The complexity to compute a single position is $O(q^3)$ where q is the number of past measurements taken into account. The maximum frequency at which this computation step is invoked is limited by the duration of a data packet transmission. As the transmission of a data packet takes 10 s the highest frequency at which algorithm 1 is called is $\mathrm{f_{max}} = 0.1$ Hz. For $q \approx 10$ the time to compute a new position is t=0.1 s on a 1 GHz PC. This makes this algorithm well suited to run on the Main Vehicle Computer of today's AUVs.

Initialize position matrix $\boldsymbol{T}(0) = [\boldsymbol{x}^A(0) \;\; c(0) = 0]$
loop {compute position}
  $m++$
  Wait for new range/position pair $\boldsymbol{x}^C(m)$,$z^C(m)$,$\boldsymbol{P}^C(m)$,$r(m)$ from CNA
  Use $z^C(m)$ to project $\boldsymbol{x}^C(m)$ to a plane at the AUV's depth $z^A(m)$
  for $j = 1$ to q **do** {Calculate intersection solution between now (m) and j steps in the past}
    $n = m - j$
    $\boldsymbol{x}_j^A(m) \leftarrow (1)|_{\boldsymbol{x}(n)^C, \boldsymbol{x}(m)^C, r(n), r(m), \boldsymbol{d}_{\overline{n,m}}}$ {Position}
    $\boldsymbol{P}_j^A(m) = \boldsymbol{J}_{n,m}\boldsymbol{G}_{n,m}\boldsymbol{J}_{n,m}^T$ {Covariance}
    $\boldsymbol{S}(m) \leftarrow \boldsymbol{x}_j^A(m), \boldsymbol{P}_j^A(m)$ {Add solution $\boldsymbol{x}_j^A(m)$ and its covariance $\boldsymbol{P}_j^A(m)$ to solution matrix:}
  end for
  for $o = 1$ to q **do** {Iterate through all past time steps}
    for $u = 1$ to q **do** {Iterate through all positions}
      for $v = 1$ to q **do** {Iterate through all solutions}
        $c_{u,v}(m-o, m) \leftarrow c_u(m-o) + (3)|_{\boldsymbol{x}_u^A(m-o), \boldsymbol{P}_u^A(m-o), \boldsymbol{x}_v^A(m), \boldsymbol{P}_v^A(m), \boldsymbol{d}_{\overline{m-o,m}}, \boldsymbol{Q}_{\overline{m-o,m}}}$
      end for
      $\boldsymbol{T}(m) \overset{c_v(m)=\min_{\forall u}(c_{u,v}(m-o,m))}{\leftarrow} [\boldsymbol{x}_v^A(m) \;\; \boldsymbol{P}_v^A(m) \;\; c_v(m)]$
    end for
  end for
  The computed position at $t(m)$ is : $\boldsymbol{x}_w^A(m) = \boldsymbol{x}_v^A(m)$ with w s. t. $c_w(m) = \min_{\forall v}(c_v(m))$
end loop

Algorithm 1: Summary of cooperative navigation algorithm.

C. Other Possible Approaches

There exist a number of alternative approaches which permit tracking of target positions in the face of uncertain position measurements. In particular, recursive Bayesian estimation is a probabilistic approach for estimating a probability density function (or more specifically an AUV position) using measurements received over time. The Kalman Filter [Kal60] is the optimal Bayesian filter for a linear system receiving measurements which are observed in Gaussian noise. A Taylor expansion of the dynamics of a non-linear system about its current mean and covariance give rise to the nonlinear Extended Kalman Filter (EKF) [Jaz70].

Recent attempts to fully recognize the difficulties of non-linear non-Gaussian filtering led to Sequential Monte Carlo, commonly known as particle filtering [DdFG00]. Particle filtering is an advanced simulation technique which avoids the assumptions mentioned above by instead directly sampling the underlying distribution. Both of these approaches are considered to be less suitable for the moving baseline navigation problem for the following reasons:

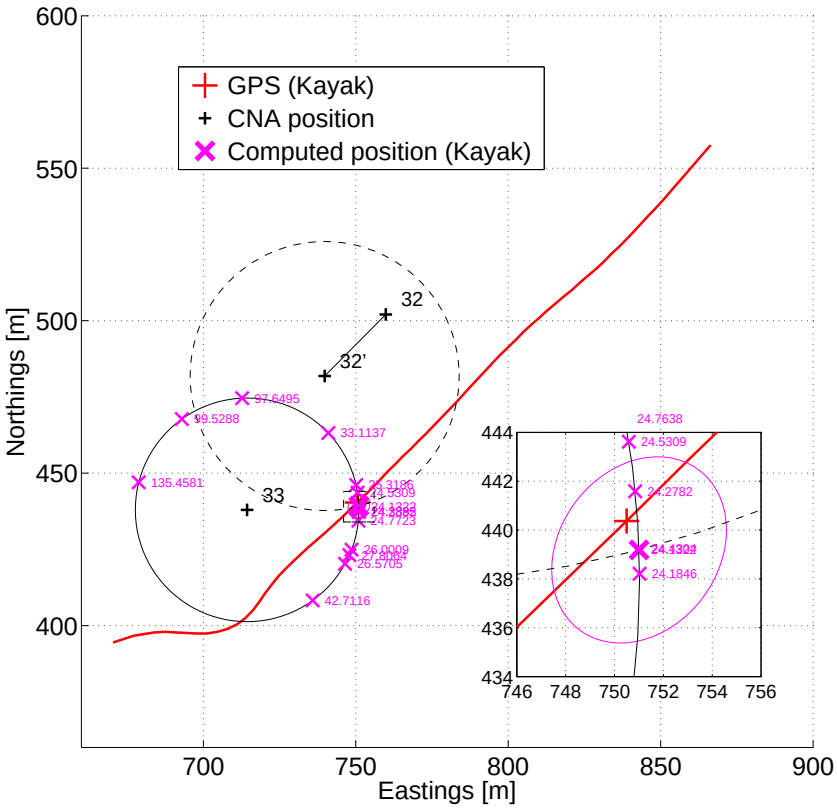

Fig. 2: All possible solutions for solution #33 with accumulated transition cost; Inset: Detailed view of selected solution and GPS ground-truth

Firstly the Kalman filter assumes measurements are distributed normally around the true mean. For the acoustic channel in water this is most certainly not the case. Signal reflections from the surface of the water as well as from temperature or salinity discontinuities within the water column itself lead to a distribution which is not only heavy-tailed but rather a complex multi-modal distribution which is difficult to model and constantly changing [VBL96]. Figure 3 shows an example of range data obtained from LBL beacons described in section I which clearly show outliers. Olson et. al [OLT04] show how the errors in time-of-flight (range) measurements do not have a Gaussian distribution.

While the WHOI acoustic modem does employ some techniques to suppress the multi-modality of the distribution, it is expected that even a single occasional outlier measurement will introduce a significant bias to the Kalman filter estimate, leading to an unacceptably long period of time for re-convergence to the correct AUV position estimate. In section IV-D and figures 11and 12 an EKF is implemented which illustrates this effect.

Secondly the multi-modal nature of the distribution could perhaps be reconciled using a particle filter. To do so with such low frequency measurements would require a large enough particle cluster to adequately sample the large

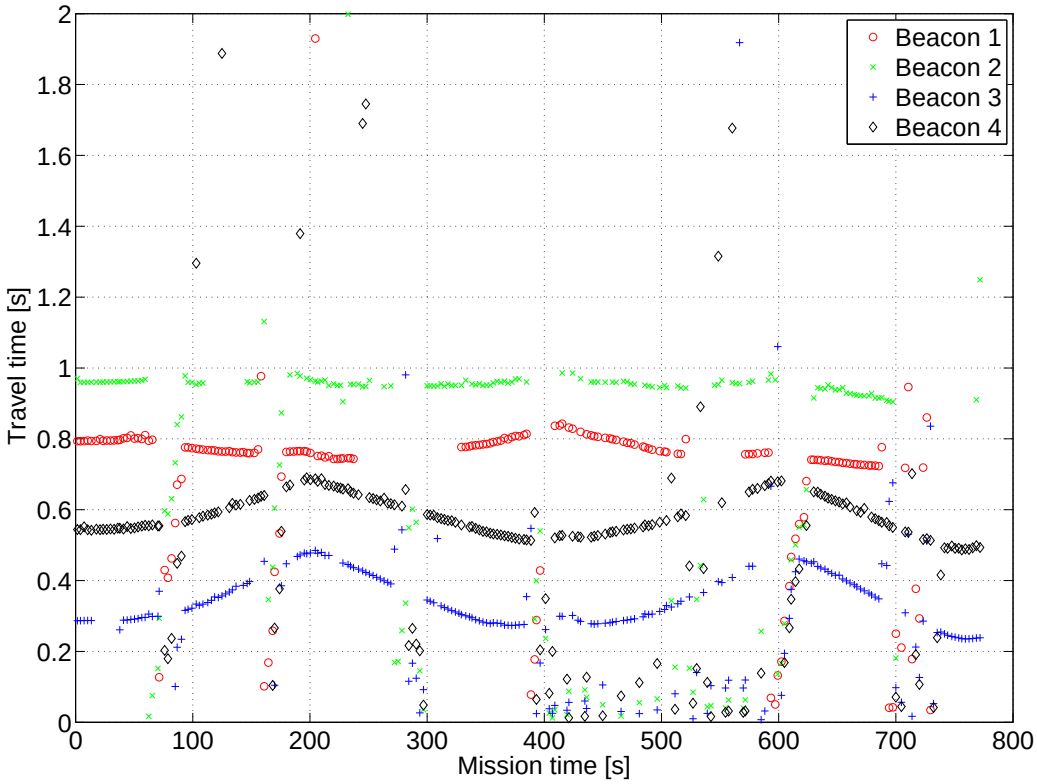

Fig. 3: Time-of-flight obtained from four LBL beacons. The plot shows significant outliers for all beacons, particularly between 400 s and 600 s

area of uncertainty that develops between corrections - an area of perhaps hundreds of meters square. It would also require the storage of the paths of each particle path — so that the correction step could be applied to the delayed state particle filter. It is considered that such an approach would be disproportionate to the problem at hand.

Again an example of particle filter-based MLBL tracking is shown in section IV-D and figures 11 and 12 with further discussion.

For these reasons, our approach proposed earlier in this section is considered to be more suitable for solving this problem.

III. Experiments

To test the algorithm we performed three separate experiments which involved different surface and underwater vehicles with very different characteristics. The first experiment using surface craft as CNAs enabled us to collect GPS position so that the algorithm's results could be compared against ground truth. The second and third experiment involved two types of underwater vehicles using a surface craft as CNA. One was a buoyancy driven glider, the other a propelled AUV. All three vehicles and their capabilities are described in the following sections.

(a) Three kayaks navigating cooperatively

(b) Towfish with modem transducer

A. Surface crafts only

The first experiment used several low-cost ASCs. The ASC is shown in Figure 4a and described in [CLV+05]. It is a kayak hull outfitted with a thruster, a mini-ATX PC, GPS and the same acoustic modem which is also used on the AUVs and glider. The vehicle dynamics of the ASC are comparable to those of a mid-sized AUV. By using only the acoustic modem to exchange information and estimate ranges between the two vehicles, we have applied the same restrictions which are encountered in an AUV-only scenario while at the same time being able to compare the algorithm's navigation performance against the "true" GPS position. Figure 4b shows the modem transducer mounted into a towfish which was hanging about 2 m below the keel.

Three ASCs were set up to run in formation along a trackline while broadcasting their position information over the acoustic modem. Each ASC in the formation was able to participate actively, by sending information, and passively by computing its position estimate based on the information obtained from the other two, but the results are only shown for one ASC of the formation. In this case two kayaks act as the "CNAs" while the other kayak acts as the "AUV" . In the setup shown in Figure 4a the center kayak ran a preprogrammed mission using its GPS for navigation. The other two kayaks followed in a predetermined formation in order to stay within range of the acoustic modems. The position/range-pairs obtained from the two CNAs over the acoustic modem were logged by the AUV-kayak and the positions were computed in post-processing.

B. Kayaks and an underwater glider

The second experiment which took place during the MB06 experiment in Monterey Bay, CA in August 2006 involved two ASCs as described in the previous section and an underwater glider operated by the Applied Physics Lab of the University of Washington (APL-UW). A glider shown in Figure 4 is a buoyancy driven vehicle. By pumping oil from an internal reservoir to an outside bladder, the glider can change its displaced volume and become

positively or negatively buoyant. A set of ”wings” adds a forward component to the otherwise purely vertical motion. The glider performs a sawtooth pattern which can take it to depths of more than 2000 m. The internal battery pack can be shifted along the longitudinal axis to provide pitch control as well as rolled around the longitudinal axis to provide yaw control in conjunction with a set of vertical fins. A detailed description of *Seaglider* can be found in [EOL+01]. The low power consumption ($\approx$ 1 W) makes for very long duration missions which can last up to half a year. While on the surface, the glider can reset its navigation using a GPS, but during the dive the very small power budget only allows for very simple navigation sensors such as a depth sensor and a compass. The information from these sensors together with a vehicle model is used to compute dead-reckoning navigation information. The position estimate derived from these sensors can drift at rate of up to 30 % of distance traveled, especially when underwater currents are present. As a result the drift rate can lead to a large cumulative navigation error during a dive which can typically last up to several hours. This makes a glider particularly suited for cooperative navigation as in a scenario with several gliders, a surfaced glider with access to GPS could provide navigation information for every submerged glider within communication range. While the power consumption of an acoustic modem is very high during transmission ($\approx$ 20 W), only a small number of these transmissions would occur while the glider is on the surface which takes place about every 2 h. In receive mode the power consumption drops to 0.1 W. As a result an acoustic modem would only add about 10-15 % to a glider’s power budget. During the MB06 experiment a modem was added to a glider for the first time. As the modem was only capable of logging information and did not have access to the gliders main vehicle computer (which provides the dead-reckoning information), on-board processing was not possible. The ASCs measured the range to the glider and by combining the logs from the kayaks, the glider’s Main Vehicle Computer and the glider’s log of the modem traffic it was possible to compute post-processed solutions of the glider’s positions. The shallow water of Monterey Bay prohibited dives deeper than 30 m. As the distance traveled in horizontal direction during a single dive is directly proportional to the maximum achievable depth, the depth limit only allowed for transsects which were about 100 m long. The main goal of the experiment was to demonstrate the feasibility of glider communication for navigation purposes. Future experiments will involve longer and deeper dives leading to longer transsects.

C. Kayaks and an AUV

During a demonstration at the *Naval Surface Warfare Center (NSWC)* in Panama City, FL, USA two ASCs and a Bluefin 12” AUV (figure 5) ran several missions where the ASCs acted as CNAs and followed the AUV while sending their GPS-derived position over the acoustic modem. The AUV also obtained distances to the transmitting ASC and stored both information for post processing. Ground truth was not directly available, but by post-processing (provided by Bluefin) data from the sophisticated and well calibrated sensor package and including the position obtained through the GPS after surfacing, accurate navigation information was available which was used to compare the results of the CN algorithm.

Fig. 4: University of Washington - Applied Physics Lab's *Seaglider*

Fig. 5: Two MIT ASCs and one Bluefin 12" AUV

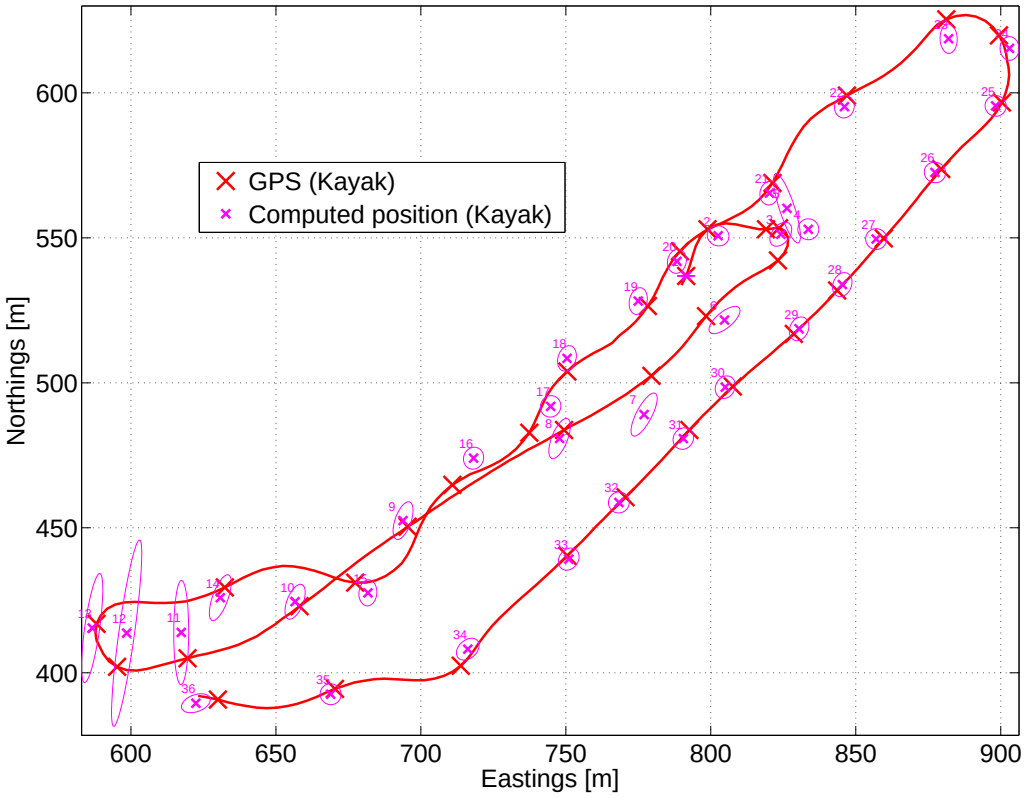

Fig. 6: GPS tracks of CNA (ASC) and computed positions

IV. Results

A. Surface crafts only

Post-processing the data logged on the ASC acting as a surrogate for an AUV we computed the position estimate whenever a broadcast from any of the two CNAs was successfully received. Figure 6 shows the GPS track of the ASC and the computed positions with their associated error ellipse. The tracks of the CNAs are not shown. Figure 7 shows the error of the computed position, the distance between the computed and the GPS position. One factor that contributes to the error are the differences in the GPS derived positions for CNA and AUV. The larger errors (solution #6, #15 and #16) are associated with large errors in the range measurements.

B. Kayaks and an underwater glider

As described earlier, the shallow depth of Monterey Bay only allowed for shallow diving depths and, as a result, very short transects of the glider. Figure 8 shows the positions of the two ASCs (acting as CNAs) as well as the dead-reckoned and computed positions of the glider. The inset shows a detailed view of the glider track (dead-

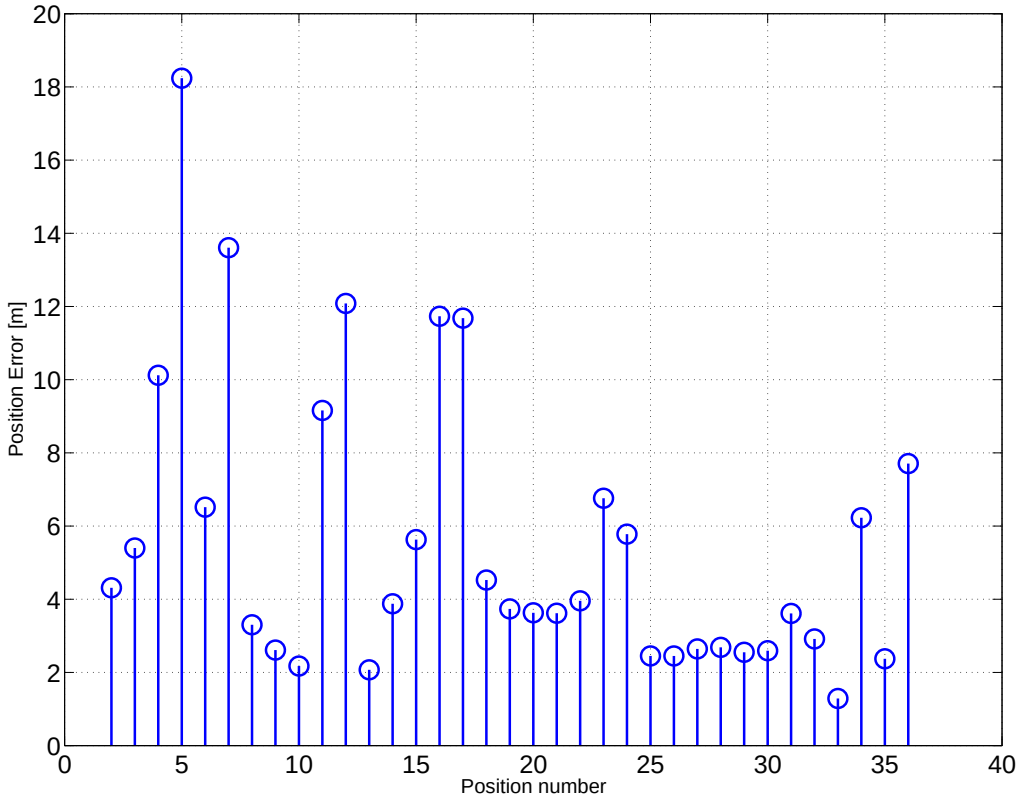

Fig. 7: Difference between GPS and computed position

reckoned and computed). The GPS fixes mark the last GPS derived position before the glider submerged as well as the first one after it surfaced. Due to the short transect the cumulative error of the dead-reckoned position is not significantly above the uncertainty of the computed position, however the computed position just before surfacing is much closer to the GPS surfacing position than the dead-reckoned one. Future experiments involving longer dives with transects of several kilometers in length should lead to significant differences between the dead-reckoned and the computed position.

C. Kayaks and an AUV

A total of 16 cooperative navigation missions were run during which the AUV received the CNA's position and measured the CNA-AUV range. During these runs the AUV acted as a master and requested a new position every 30 seconds switching between the two CNAs. Of all positions requested the AUV would receive about 60 %. For the remaining 40 % of the queries the CNA did either not receive the request or the AUV did not receive the CNA's answer. Sometimes the AUV would also suspend requesting positions because it needed to transfer other mission

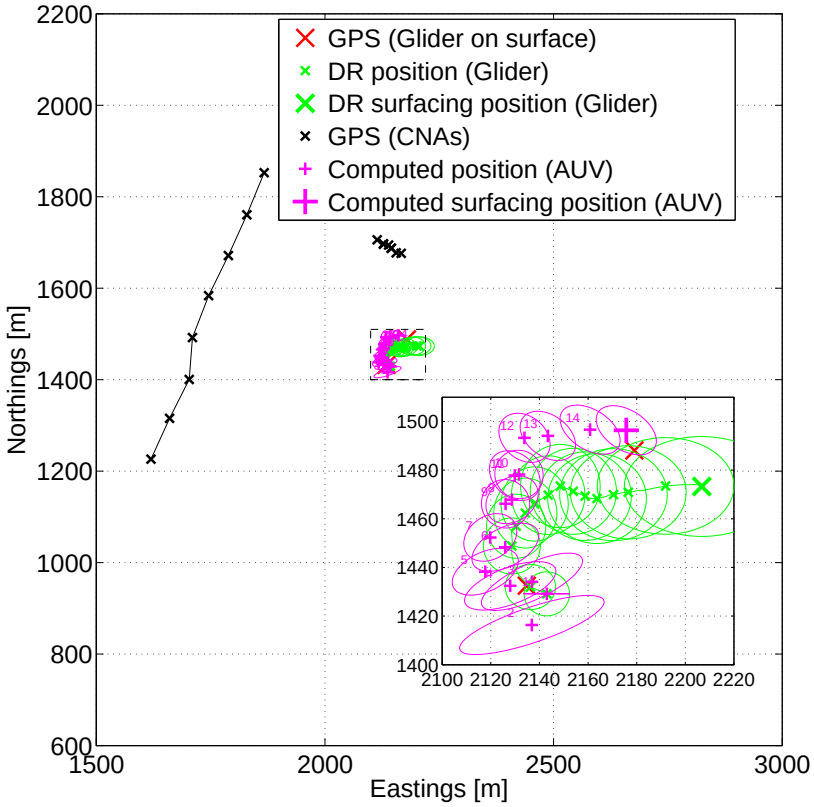

Fig. 8: Glider/ASC mission: GPS positions of CNAs and dead-reckoned and computed positions of glider; Inset: Glider positions only

specific information over the acoustic modem. As a result the update rate for position/range pairs was about one per minute.

After requesting a position/range from both CNAs, the AUV would send its own position estimate over the acoustic modem. Furthermore, the CNAs would continuously broadcast their GPS-derived position over the radio such that both CNAs were aware of where the other one is. Knowing where the AUV and the other CNA is, enabled the CNAs to follow the AUV in a way that was optimal for cooperative navigation:

- In order to maintain optimal acoustic communication, the AUV would try to stay 150 m behind the AUV.
- To minimize the covariance of the computed solution the CNAs would try to form a right-angled triangle with the AUV in the corner with the right angle and the CNAs in the other two.

As the AUV's position updates were received at a rate of only $O(1/\text{min})$, it was very difficult for the CNAs to maintain the triangular formation when the straight transects were short (Figure 9). During the second mission (Figure 10) CNA1 was able to maintain an aft-starboard position with respect to the AUV while, CNA2 maintained

an aft-port position. Even when the formation was not maintained the AUV's broadcast enabled the CNAs to stay close enough to maintain the acoustic communication channel. The navigation error was modeled using sensor noise as provided in [Eus05]. While the results for only two runs are shown in figure 9 and figure 10 the quality of the results computed by the algorithm was the same for all 16 runs.

Figure 9 and Figure 10 show two of the missions carried out. The first mission consisted of a U-shaped trackline of about 1 km length. After initializing its position with GPS the AUV submerged to a depth of about 12 m and ran the mission at a constant speed of 1.5 m/s. The detail in Figure 9 shows the computed position #8 and its covariance ellipse. Also shown is the "ground-truth" track as well as the "ground-truth" position estimate at the time of the computed solution. As the "ground-truth" position is based on post-processed dead-reckoning data the distance between it and the computed position can only provide a qualitative assessment of the algorithm's performance. As a result we did not compute the Euclidean distance between the two positions. Also, the post-processed track is the result of a non-linear optimization so no covariance estimate can be provided.

The second mission consisted of a 4 km east-to-west trackline. During this mission the kayaks were able to maintain the triangular formation for most of the time. On five occasions during this mission the AUV would spend four minutes transmitting mission specific data. During this time no positions were queried from the CNA which lead to the wide gaps between the computed solutions (e.g. between #19 and #20 as well as #27 and #28). The two insets in figure 10 show two magnified views of the track at the same scale. The bottom one near the beginning (eastern end) of the mission and the top one of the end (west). These illustrate how beneficial the information from the CNAs is for navigation accuracy. In the beginning the dead-reckoned position is very close to the "ground-truth" and the computed solution while at the end of trackline the "ground-truth" as well as the computed position have consistently moved away from the dead-reckoned position. The dead-reckoning error, represented by the growing error ellipse, depends on the distance traveled and will grow without bound if the AUV is submerged, while the error of the computed solution only depends on the position error of the CNAs and the geometry. It is bounded if the position error of the CNAs is bounded and if positions which were computed from collinear or near collinear geometries are filtered out. Toward the end of the second mission, the CNAs were not able to keep up with the AUV which lead to a less favorable geometries resulting in slightly larger error covariances of the computed solution than in the beginning. As in the first mission, the algorithm's performance is hard to quantify. Qualitatively, the computed solutions are consistently very close to the "ground-truth" throughout the entire track.

D. Comparison with Bayesian Estimators

In order to compare the performance of our CN algorithm with common classical approaches, an EKF and a particle filter with 300 particles, we computed the position using all three methods at each time instant k when a new range/position pair was available. Because of the high quality dead-reckoning measurements and absence of range measurements outliers in the available kayak/AUV data sets, each of the three methods performed similarly and the results were within the accuracy of the ground truth.

Large underwater range measurement outliers can occur in more challenging experimental scenarios. In such

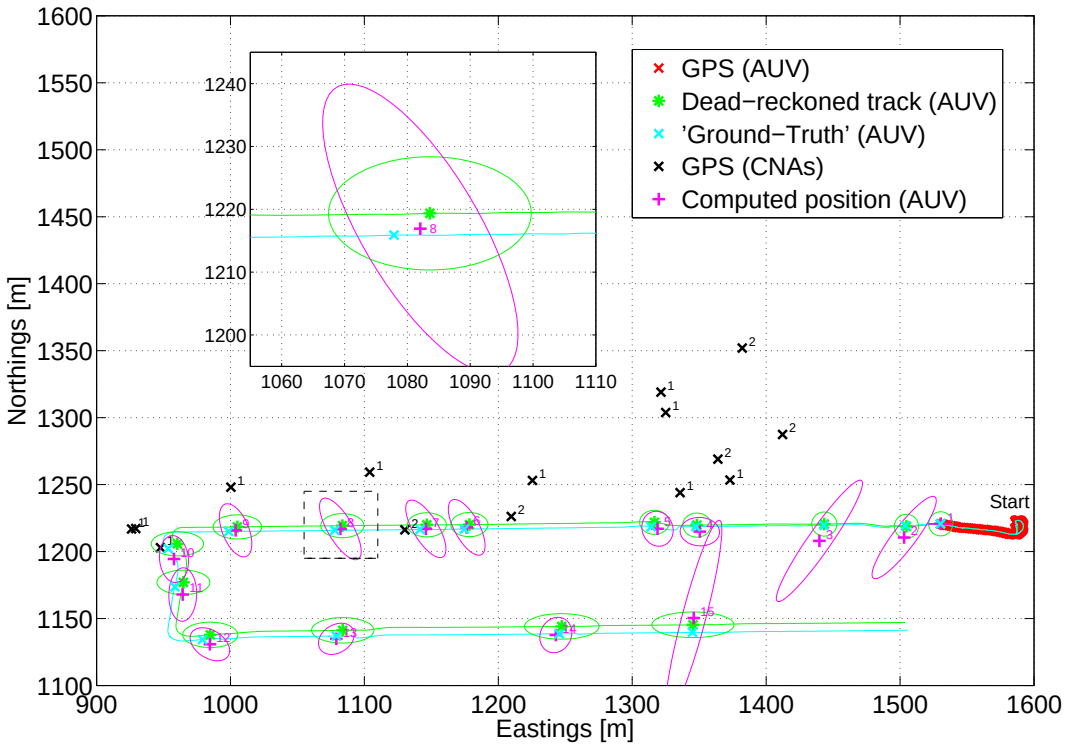

Fig. 9: AUV/ASC mission 1: Dead-reckoned track and computed positions of AUV, GPS positions of CNAs; Inset: Detailed view of position #8

a scenario the Gaussian noise assumption does not hold [OLT04]. For this reason we simulated a typical outlier measurement by setting the range measurement obtained by the AUV at $k = 5$ from $r(5)$ =116.86 m to $r(5)$ =60 m. All subsequent range measurements were unchanged. The computed tracks are shown in figure 11. Upon receipt of the fifth measurement the error of the position estimate "jumps" for all three methods, most significantly for the CN algorithm. However at $k = 6$ the CN algorithm instantly recovers to the correct position, while the EKF and particle filter slowly converge towards the correct path. This is due to the very low measurement update frequency. The erroneous position produced by our CN algorithm at $k = 5$ is particularly large because our approach may only select from the solution set provided in $\boldsymbol{S}(5)$. This range measurement is however inconsistent with the previous range measurements and the dead-reckoned track and as a result has a much higher accumulated cost $\mathcal{C}(5)$, shown as a single peak in figure 12. Therefore it would be possible to use $\mathcal{C}$ to detect and filter out false range measurements.

In summary an EKF in unsuitable for this application. However a more advanced particle filter with a sufficiently large number of particles could possibly provide similar performance to our proposed algorithm.

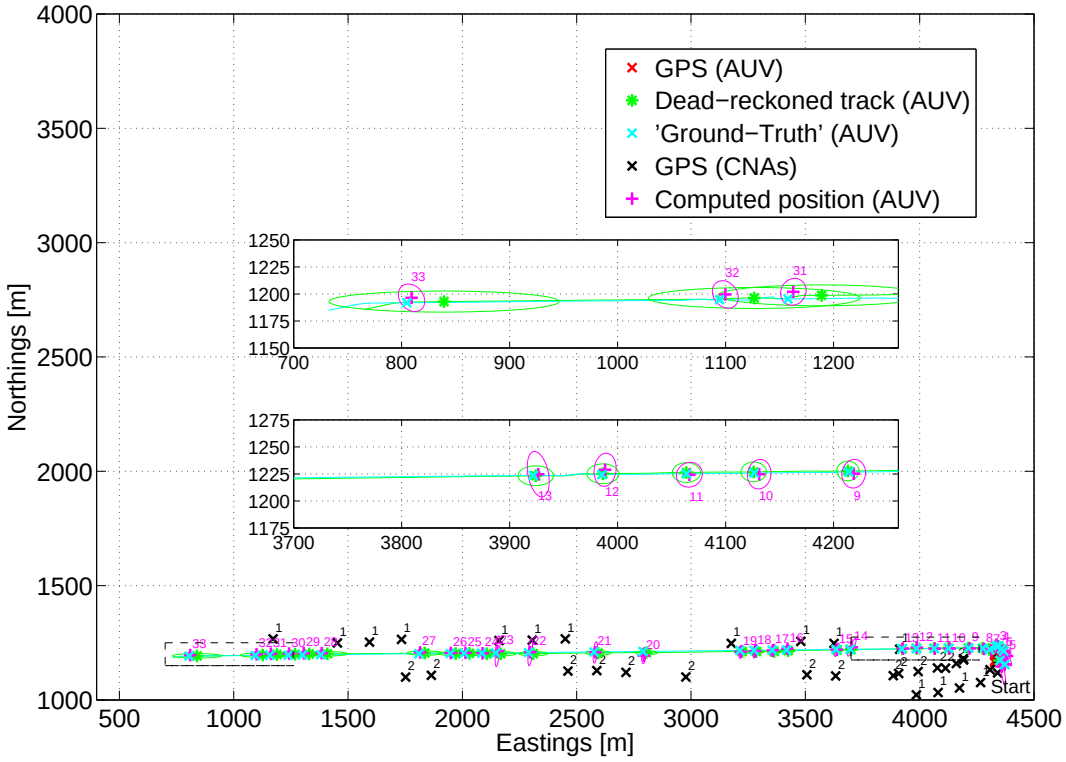

Fig. 10: AUV/ASC mission 2: Dead-reckoned track and computed positions of AUV, GPS positions of CNAs; Inset (top): Detailed view of mission end (positions #31, #32 and #33) ; Inset (bottom): Detailed view of mission start (positions #9 through #13)

V. Conclusion

This paper has described a new algorithm for cooperative navigation of AUVs and described its experimental validation in a sequence of experiments using a variety of autonomous marine platforms.

The algorithm is particularly well suited for underwater applications where the communication bandwidth is severely limited and only range information is available. By taking a large set of past range measurements into account during each computation, the algorithm can recover after a range-measurement outlier. As the bandwidth of the acoustic modems limits the rate at which new exteroceptive measurements are available and thereby the computation of a new position estimate is invoked, this algorithm is computationally very inexpensive and well suited to run concurrently on the Main Vehicle Computer of all underwater platforms. The information which needs to be obtained from other vehicles is often transmitted as part of a telemetry or mission-specific message, so no extra bandwidth needs to be allocated to transmit information specifically for cooperative navigation.

A novel feature of these experiments is that they utilize the MIT SCOUT autonomous surface craft (ASC) as

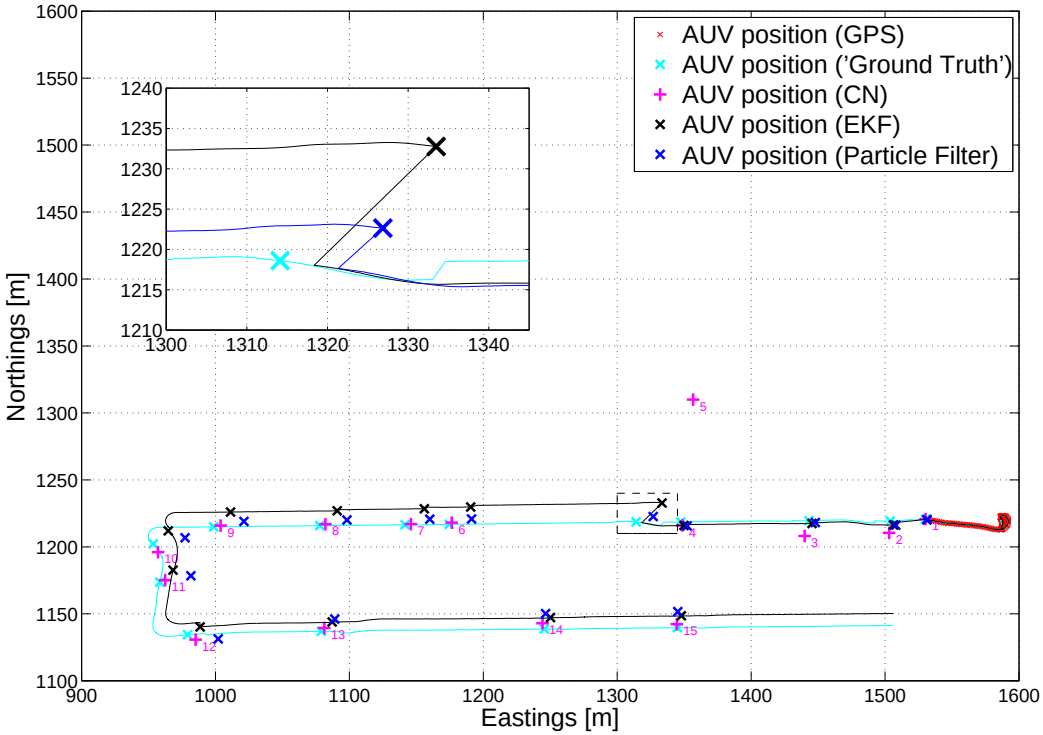

Fig. 11: AUV/ASC mission 2 with falsified range measurement at $k = 5$: The erroneous range measurement causes a localization error for all 3 algorithms at $k = 5$, but while the CN algorithm has fully recovered at the next step, EKF and particle filter only converge slowly towards the correct solution.

mobile platforms. While several other researchers have performed experiments with an individual ASC [VROSM96], [Man97], [MMCW00], we believe that ASCs offer extremely powerful capabilities when operated together in mobile vehicle networks. The use of an ASC network for cooperative AUV research is akin to using training wheels to ride a bike; GPS and WiFi communications greatly ease software development for tasks such as formation-keeping. The cost, complexity, and risk of these experiments are at least an order of magnitude less than similar experiments would be with AUVs. GPS measurements also provide a convenient ground truth for the trajectory estimation process.

In the evolution of our work, initial experiments using only surface craft were essential for the early development of the approach. Subsequently, we were able to add two different types of platforms to operate with two ASCs, a buoyancy-driven undersea glider and a conventional AUV. In each scenario, we were able to show the effectiveness of our algorithmic approach. In all runs for all scenarios the algorithm computed vehicle positions which were close to the ground-truth where available or consistent with available navigation information such as dead-reckoning and

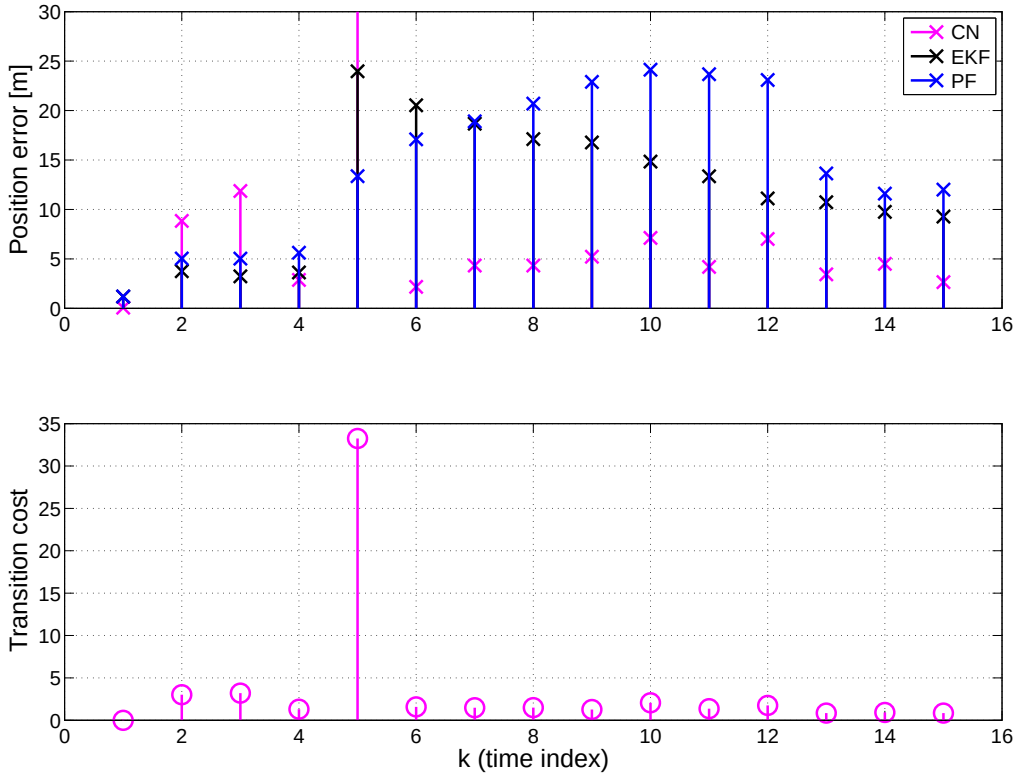

Fig. 12: Position error for CN, EKF and Particle Filter for the tracks shown in figure 11: Top: position error for CN, EKF and Particle filter. Bottom: cost function for CN showing a very large peak at $k = 5$ which would enable one to filter out this inconsistent range measurement

GPS surfacings.

A number of issues remain for future research in this area. One important topic is to address adaptive motion control for the group of AUVs. Clearly, the mobile network can achieve better positioning accuracy if the platforms are able to execute favorable trajectories, however, one must also take into account mission objectives. An interesting objective would be to develop methods that concurrently optimize the coverage achieved by a group of vehicles doing a task such as surveying an unknown environment, while simultaneously maintaining connectivity of the network and minimizing position errors.

Future experimental work is necessary to implement the algorithm in a larger network, with more than three vehicles, to study fully the scaling properties and bandwidth utilization of the algorithm. Finally further work will consider a comparison between the proposed algorithm and Bayesian estimators discussed in section IV-D. Nonetheless we believe that the experiments reported here provide good evidence that the proposed algorithm provides an effective approach to cooperative navigation of AUVs for a large class of missions, especially search and survey

of large areas without reliance on pre-deployed acoustic transponders.

ACKNOWLEDGMENTS

The authors wish to thank the people who helped throughout the various experiments. Joseph Curcio, Andrew Patrikalakis and Robert Williams for preparing and deploying the ASCs at the ONR UUVFest held in June 2005 at Keyport, WA. Also Jim Luby, Bruce Howe and Mike Boyd for their support during the joint ASC/glider operations in Monterey, CA in August 2006 and Jerome Vaganay, Matt Lockhardt and Joseph Daverin from Bluefin for running the 12" AUV at *NSWC* Panama City, FL in December 2006 as well as Iuliu Vasilescu. This work was supported in part by ONR grants N00014-02-C-0210, N00014-97-1-0202 and N00014-05-G-0106, and by the MIT Sea Grant College Program under grant NA86RG0074 (project RD-24).

REFERENCES

[Cat90] J. Catipovic. Performance limitations in underwater acoustic telemetry. *IEEE J. Ocean Engineering*, 15(3):205–216, July 1990.

[CLV+05] J. Curcio, J. Leonard, J. Vaganay, A. Patrikalakis, A. Bahr, D. Battle, H. Schmidt, and M. Grund. Experiments in moving baseline navigation using autonomous surface craft. In *Proc. MTS/IEEE Oceans 2005*, pages 290–294, Washington, DC, USA, September 2005.

[DdFG00] Arnaud Doucet, Nando de Freitas, and Neil Gordon, editors. *Sequential Monte Carlo methods in practice*. Springer-Verlag, 2000.

[DKSZ06] Joseph Djugash, George Kantor, Sanjiv Singh, and Wei Zhang. Range-only slam for robots operating cooperatively with sensor networks. In *Proc. International Conference on Robotics and Automation*, May 2006.

[EOL+01] C.C. Eriksen, T.J. Osse, T. Light, R.D. Wen, et al. Seaglider: a long-range autonomous underwater vehicle for oceanographic researc. *IEEE J. Ocean Engineering*, 26:424–436, October 2001.

[Eus05] R. Eustice. *Large-Area Visually Augmented Navigation for Autonomous Underwater Vehicles*. PhD thesis, Massachusetts Institute of Technology, Cambridge, MA, USA, June 2005.

[EWSG07] Ryan M. Eustice, Louis L. Whitcomb, Hanumant Singh, and Matthew Grund. Experimental results in synchronous-clock one-way-travel-time acoustic navigation for autonomous underwater vehicles. In *Proc. IEEE Intl. Conf. Robotics and Automation*, Rome, Italy, April 2007.

[FJG+01] L. Freitag, M. Johnson, M. Grund, S. Singha, and J. Preisig. Integrated acoustic communication and navigation for multiple UUVs. In *Proc. MTS/IEEE Oceans 2001*, pages 290–294, Honolulu, HI, USA, September 2001.

[GSSK06] B. Grocholsky, E. Stump, P. Shiroma, and V. Kumar. Control for localization of targets using range-only sensors. In *Proc. 10th International Symposium on Experimental Robotics (ISER)*, Rio de Janeiro, Brasil, July 2006.

[Jaz70] Andrew H. Jazwinski. *Stochastic Processes and Filtering Theory*. Academic Press, April 1970.

[Kal60] Rudolph Emil Kalman. A new approach to linear filtering and prediction problems. *Transactions of the ASME - Journal of Basic Engineering*, 82(Series D):35–45, 1960.

[KB00] D. B. Kilfoyle and A. B. Baggeroer. The current state-of-the-art in underwater acoustic telemetry. *IEEE J. Ocean Engineering*, 25(1):4–27, 2000.

[KNH94] R. Kurazume, S. Nagata, and S. Hirose. Cooperative positioning with multiple robots. In *Proc. IEEE International Conference in Robotics and Automation*, pages 1250–1257, Los Alamitos, CA, USA, May 1994.

[LHDS06] Elizabeth Liao, Geoffrey Hollinger, Joseph Djugash, and Sanjiv Singh. Preliminary results in tracking mobile targets using range sensors from multiple robots. In *The 8th International Symposium on Distributed Autonomous Robotic Systems*, pages 125–134, June 2006.

[LPL+07] N. Leonard, D. Paley, F. Lekien, R. Sepulchre, D. Fratantoni, and R. Davis. Collective motion, sensor networks and ocean sampling. *Proceedings of the IEEE*, January 2007. Special issue on the emerging technology of networked control systems.

[Man97] J. E. Manley. Development of the autonomous surface craft ACES. In *IEEE Oceans*, 1997.

[MLRT04] D. Moore, J. Leonard, D. Rus, and S. Teller. Robust distributed network localization with noisy range measurements. In *SenSys '04: Proceedings of the 2nd international conference on Embedded networked sensor systems*, pages 50–61, New York, NY, USA, 2004. ACM Press.

[MMCW00] J. E. Manley, A. Marsh, W. Cornforth, and Wiseman. Evolution of the autonomous surface craft autocat. In *IEEE Oceans*, 2000.

[OLT04] E. Olson, J. Leonard, and S. Teller. Robust range-only beacon localization. In *Proc. IEEE/OES Autonomous Underwater Vehicles*, pages 66–75, 17–18 June 2004.

[RB00] S.I. Roumeliotis and G.A. Bekey. Synergetic localization for groups of mobile robots. In *Proc. 39th IEEE Conference on Decision and Control*, pages 3477–3482, Sydney, Australia, December 2000.

[RDM02] Ioannis M. Rekleitis, Gregory Dudek, and Evangelos Milios. Multi-robot cooperative localization: A study of trade-offs between efficiency and accuracy. In *IEEE/RSJ/ International Conference on Intelligent Robots and Systems*, Lausanne, Switzerland, October 2002. IEEE/RSJ.

[Tho01] H. Thomas. Commercial offer: GPS intelligent buoy system (A.C.S.A., `http://www.underwater-gps.com`), 2001.

[VBL96] J. Vaganay, J. G. Bellingham, and J. J. Leonard. Outlier rejection for autonomous acoustic navigation. In *Proc. IEEE Int. Conf. Robotics and Automation*, pages 2174–2181, April 1996.

[VLCW04a] J. Vaganay, J. Leonard, J. Curcio, and S. Willcox. AOFNC - experimental validation of the moving long base line navigation concept. In *AUV 2004*, pages 555–556, Nagoya, Japan, June 2004.

[VLCW04b] J. Vaganay, J.J. Leonard, J.A. Curcio, and J.S. Willcox. Experimental validation of the moving long base-line navigation concept. *Autonomous Underwater Vehicles, 2004 IEEE/OES*, pages 59–65, June 2004.

[VROSM96] T Vaneck, C. Rodriguez-Ortiz, M. Schmidt, and J. Manley. Automated bathymetry using an autonomous surface craft. *Navigation: Journal of the Institute of Navigation*, 43(4), 1996.

[WYSH00] L.L. Whitcomb, D.R. Yoerger, H. Singh, and J. Howland. Advances in Underwater Robot Vehicles for Deep Ocean Exploration: Navigation, Control and Survery Operations. In *The Ninth International Symposium on Robotics Research*, Springer-Verlag, London, 2000.